JACS
JOURNAL OF THE AMERICAN CHEMICAL SOCIETY
pubs.acs.org/JACS
Communication

A Solid Zn-Ion Conductor from an All-Zinc Metal–Organic Framework Replete with Mobile Zn^{2+} Cations

Andrei Iliescu, Justin L. Andrews, Julius J. Oppenheim, and Mircea Dincă*

Cite This: J. Am. Chem. Soc. 2023, 145, 25962–25965
Read Online

ABSTRACT: We describe the synthesis and properties of $Zn_3[(Zn_4Cl)_3(BTT)_8]_2$ (ZnZnBTT, BTT^{3-} = 1,3,5-benzenetristetrazolate), a heretofore unknown member of a well-known, extensive family of metal–organic frameworks (MOFs) with the general formula $M^{II}_3[(M^{II}_4Cl)_3(BTT)_8]_2$, which adopts an anionic, sodalite-like structure. As with previous members in this family, ZnZnBTT presents two crystallographically distinct metal cations: a skeletal Zn^{2+} site, fixed within $Zn_4Cl(tetrazole)_8$ secondary building units (SBUs), and a charge-balancing Zn^{2+} site. Self-assembly of ZnZnBTT from its building blocks has remained elusive; instead, we show that ZnZnBTT is readily accessed by quantitative postsynthetic exchange of all Mn^{2+} ions in MnMnBTT with zinc. We further demonstrate that ZnZnBTT is a promising Zn-ion conductor owing to the mobile charge-balancing extra-framework Zn^{2+} cations. The new material displays a Zn-ion conductivity of $\sigma = 1.15 \times 10^{-4}$ S/cm at room temperature and a relatively low activation energy of $E_a = 0.317$ eV, enabling potential applications in the emerging field of quasi-solid-state zinc-ion batteries.

Zinc-ion batteries (ZIBs) have emerged as promising alternatives to lithium-ion batteries (LIBs) thanks to their attractive electrochemical properties, as well as their low cost, ease of manipulation, and relative safety compared to LIBs.[1−4] However, current state-of-the-art ZIBs rely on aqueous electrolytes challenged by poor reversibility, fast capacity fading, low Coulombic efficiency, dendrite growth during Zn plating/stripping, a narrow electrochemical stability window (~1.23 V), and sustained water consumption.[1,5−9] Solid-state ZIBs, employing quasi-solid or solid-state electrolytes, provide an attractive alternative to aqueous ZIBs by potentially offering increased electrochemical stability windows, higher zinc transference numbers, superior thermal stability, higher mechanical strength, and increased safety.[6,9,10]

Owing to their intrinsic porosity and permanent channels offering conduits for ion transport, metal–organic frameworks (MOFs) are attractive candidates for the fabrication of solid-state electrolytes.[11−13] In particular, MOFs' modularity and designability in terms of pore size, structure, and chemical composition allow for the methodological investigation of structure–function correlations and optimization of zinc-ion conductivity.[14−16] To promote high zinc-ion mobility in a MOF, we envisioned a negatively charged framework, charge-balanced by loosely bound Zn^{2+} cations. We hypothesized that the versatile family of MOFs comprised of the BTT linker (BTT^{3-} = 1,3,5-benzenetristetrazolate, Figure 1a) and divalent metal cations, M^{II}, with the general formula $M^{II}_3[(M^{II}_4Cl)_3(BTT)_8]_2$ (MMBTT) and a sodalite-like structure could provide an effective platform for ionic conductivity; the anionic framework is charge-balanced by M^{II} cations that sit in well-defined extra-framework positions that serve no structural role and are potentially mobile.[17−21] In particular, we identified ZnZnBTT as a promising zinc-ion conductor. However, despite the wide scope of divalent metals reported to generate the MMBTT structure-type, including almost all divalent 3d metal cations (Cr,[17] Mn,[18] Fe,[19] Co,[20] Ni,[20] Cu[21]) and Cd,[20] the analogous ZnZnBTT structure has remained elusive. In fact, prior investigations of direct solvothermal reactions between H_3BTT and $ZnCl_2$ reported the formation of three different MOFs with topologies distinct from the desired MMBTT structure, none of which presented potentially mobile Zn ions.[22]

Herein, we report the synthesis and characterization of a missing member of the MMBTT family, ZnZnBTT (Figure 1), and investigate its Zn-ion transport and dynamics. Because direct solvothermal reaction between the free ligand H_3BTT and Zn^{2+} salts failed to deliver the desired anionic sodalite-type structure, we reasoned that postsynthetic metal exchange (PSME) starting from one of the existing MMBTT materials may instead be able to generate ZnZnBTT. Indeed, this family of MOFs has long been known to engage in cation exchange, including complete exchange of even the skeletal cations in some cases.[20,23]

In this context, MnMnBTT is a particularly attractive starting material for exchanging with zinc ions: (1) it is known to engage at least partially in metal exchanges, including with Zn^{2+},[23−25] and (2) Mn^{2+} sits at the bottom of the Irving–Williams kinetic stability series, which should make it particularly prone to exchange with other ions.[26] Indeed, we reasoned that the transformation of MnMnBTT into ZnZnBTT should be thermodynamically favorable and that

Received: September 19, 2023
Revised: November 8, 2023
Accepted: November 20, 2023
Published: November 27, 2023

https://doi.org/10.1021/jacs.3c10326
J. Am. Chem. Soc. 2023, 145, 25962–25965

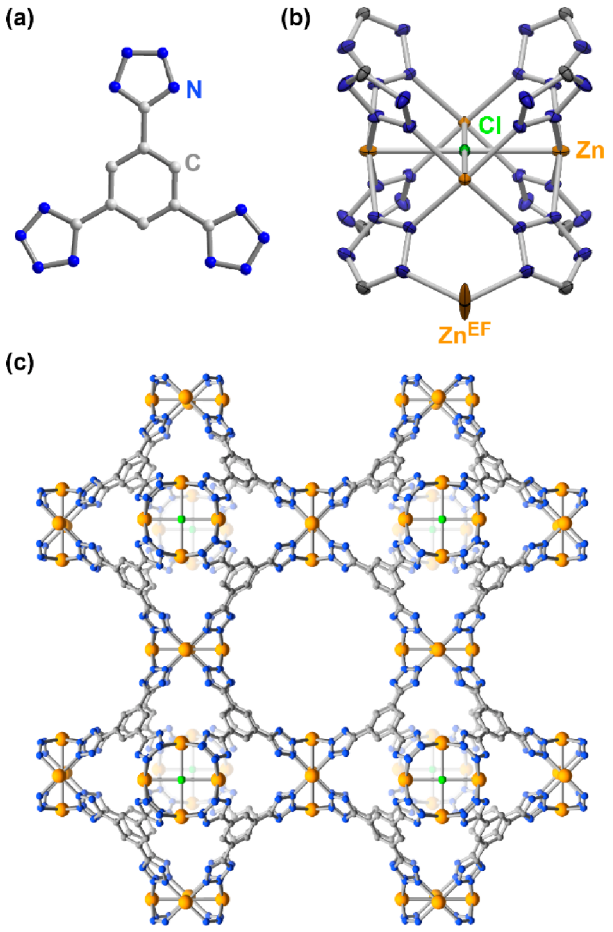

Figure 1. (a) Ball-and-stick representation of the tritopic 1,3,5-benzenetristetrazole (H_3BTT) linker. (b) Solid state structure of the SBU of ZnZnBTT formed by a $[Zn_4Cl]^{7+}$ core and eight bridging tetrazolate rings at 100 K depicted at 50% displacement ellipsoid probability. One of the eight symmetry-equivalent C_s-symmetric extra-framework (EF) Zn^{2+} (Zn^{EF}) positions is highlighted. (c) Ball-and-stick representation of the sodalite-like structure of ZnZnBTT. Hydrogen atoms, solvent molecules and charge-balancing extraframework Zn atoms are omitted for clarity.

previously reported Mn-to-Zn metal exchanges in this system were kinetically limited.

Soaking as-synthesized crystals of MnMnBTT in a 1.75 M methanolic solution of $ZnCl_2$ for 3 days at 80 °C under a nitrogen atmosphere generates the isoreticular ZnZnBTT structure as air-stable, colorless single crystals, suitable for X-ray diffraction (Figures 1 and S1, Table S1). The Zn:Mn molar ratio was measured over the course of the reaction via inductively coupled plasma mass spectrometry (ICP-MS) to monitor the extent of metal exchange. ICP-MS data confirmed that Zn incorporation reached >99% after 48 h and >99.9% after 72 h, when the reaction was considered complete. X-ray photoelectron spectroscopy (XPS) confirmed the incorporation of Zn in the product and the removal of Mn to subdetection limit values (Figure S3).

ZnZnBTT crystallizes in the cubic $Pm\bar{3}m$ space group, with a unit cell length of a = 18.8626(3) Å (Table S1). The slight contractions of the unit cell, metal−N(linker) and metal−Cl bonds in ZnZnBTT, compared to MnMnBTT, are attributed to the lower effective ionic radius of Zn^{2+}, compared to Mn^{2+} (Figure S2, Table S2). As other members in the MMBTT family, ZnZnBTT is comprised of $[Zn_4Cl]^{7+}$ secondary building units (SBUs), a cluster type that is nevertheless unprecedented for Zn, defined by a square planar μ_4-chloride anion and eight BTT^{3-} linkers. The overall anionic $[(Zn_4Cl)_3(BTT)_8]^{3-}$ repeating unit is charge-balanced by extra-framework Zn^{2+} (Zn^{EF}) cations, which occupy well-defined, locally C_s-symmetric positions between the N(1)/N(4) positions of tetrazole rings of adjacent BTT^{3-} linkers (Figure 1b). The occupancy of the extra-framework C_s-symmetric Zn^{2+} position was refined independently during single-crystal structure determination; the excess Zn^{2+} occupancy found is attributed to an additional 5.2 equiv of $ZnCl_2$ that occupy available binding sites and are indistinguishable from Zn^{EF} sites. Therefore, a more precise molecular formula of as-synthesized ZnZnBTT can be assigned as $Zn_3[(Zn_4Cl)_3(BTT)_8]_2 \cdot 5.2\ ZnCl_2$, guest solvent equivalents notwithstanding. This formula is corroborated by the intra-framework to extra-framework Zn ratio calculated by XPS (Figure S3, Table S3). Powder X-ray diffraction (PXRD) confirmed the bulk phase purity of ZnZnBTT (Figure S4). Although the parent MnMnBTT material decomposes under air within days, as-synthesized ZnZnBTT is benchtop stable at room temperature, as confirmed by retention of crystallinity after 2 months under air (Figure S4). In line with extra $ZnCl_2$ equivalents partially occupying the pore volume, a Brunauer−Emmett−Teller fit to the N_2 adsorption isotherm for ZnZnBTT at 77 K (Figures S5, S6) gave an apparent surface area of 958 m^2/g, lower than that of the parent material. The N_2 total pore volume was found to be 0.37 cm^3/g. We note that in its activated form ZnZnBTT decomposes quickly when exposed to air, likely via bond hydrolysis caused by moisture.

For the purposes of Zn-ion conductivity, we reasoned that the extra $ZnCl_2$ equivalents, along with the Zn^{EF} cations, might together provide a sufficiently high carrier concentration to promote efficient Zn-ion transport. Carrier migration would occur via the C_s-symmetric tetrazole binding pockets (Figure 1b). To facilitate the migration of Zn^{2+} cations within the pores of the MOF, as well as between different MOF crystallites, propylene carbonate (PC) was used as a secondary electrolyte. To test Zn ion mobility, as-synthesized ZnZnBTT was soaked in neat PC and dried to form ZnZnBTT-PC. We note that after drying, ZnZnBTT-PC still behaves as a free-flowing powder. ZnZnBTT-PC was pressed into a pellet and sandwiched between two stainless steel (SS) electrodes in an electrochemical cell. To measure the ionic conductivity of the material, the SS|ZnZnBTT-PC|SS cell was subjected to potentiostatic electrochemical impedance spectroscopy (PEIS) in the frequency range 500 kHz−500 Hz. A fit of the PEIS data to the appropriate equivalent circuit (Figures S7) provided a room-temprature conductivity value of $\sigma = 1.4 \times 10^{-6}$ S/cm for as-synthesized ZnZnBTT-PC, establishing ZnZnBTT as a promising quasi-solid-state electrolyte. Importantly, PXRD confirmed that ZnZnBTT maintains crystallinity following the electrochemical measurements (Figure S4). Moreover, we confirmed that the conductivity measured via PEIS corresponds to ion mobility within the material by measuring the electronic conductivity of the ZnZnBTT material as 7×10^{-10} S/cm (Figure S8), several orders of magnitude lower than the ionic conductivity, as expected given the structure of the framework. Therefore, we attribute the conductivity of ZnZnBTT-PC to the loosely bound extra-framework Zn^{2+} cations that are able to hop between equivalent positions within the framework. In

https://doi.org/10.1021/jacs.3c10326
J. Am. Chem. Soc. 2023, 145, 25962−25965

addition, we demonstrated that ZnZnBTT-PC is stable under a wide potential window of more than 2 V vs Zn metal, rendering the material suitably stable under zinc-ion battery operating conditions (Figure S9).

Several variables can be optimized to further increase the Zn mobility. As might be expected, initial conductivity measurements for as-synthesized ZnZnBTT revealed that its performance depends on multiple factors, including the degree of desolvation during activation, loading of the PC secondary electrolyte, and thermal treatment of the PC-soaked material. Upon optimizing for these variables, we found that ZnZnBTT·5.2 $ZnCl_2$ exhibits the highest room temperature conductivity after (i) thermal activation under dynamic vacuum for at least 18 h at 150 °C, (ii) pelletization, (iii) wetting with an equal amount of PC by mass, and (iv) heating the ZnZnBTT-PC composite to 100 °C for ∼18 h, before measuring the conductivity. For this champion device, the 25 °C conductivity was found to be 1.15×10^{-4} S/cm (Figure S10), much higher than conductivities found for dense Zn-ion solid state electrolytes, and comparing favorably with the best MOF-based electrolytes.[14−16,27] Variable temperature PEIS conducted on this champion cell between 25 and 75 °C (Figure S11, Table S4) gave an activation energy for ion diffusion of E_a = 0.317 eV (Figure 2b), in line with those found for other fast Zn ion solid electrolytes.[16]

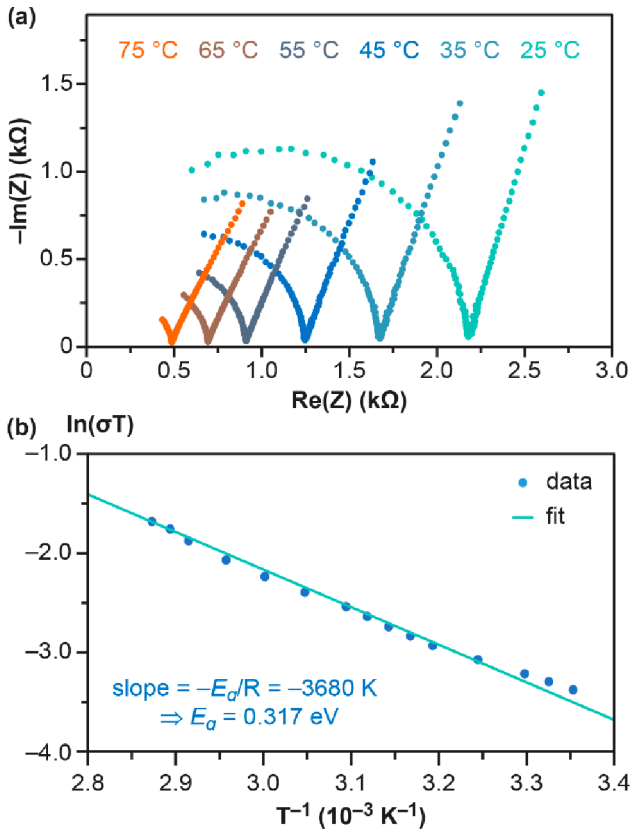

Figure 2. (a) Potentiostatic electrochemical impedance spectra (PEIS) of ZnZnBTT-PC at selected temperatures, shown as Nyquist plots. (b) Linearized temperature-dependence of the ionic conductivity of ZnZnBTT-PC, fitted to the linearized Nernst−Einstein relation (see Supporting Information). The linear model was used to calculated the activation energy of ion diffusion in ZnZnBTT as 0.317 eV.

The foregoing results add to a growing body of evidence toward the utility of MOFs as potential Zn-ion electrolytes. From a purely synthetic perspective, the isolation of previously unknown ZnZnBTT within a broader family of well-known sodalite-like frameworks highlights PSME as a powerful tool for accessing new MOF structures, allowing for decoupling the choice of topology from the choice metal. Here, the rational targeting of an anionic framework that supports a high concentration of mobile Zn^{2+} ions led to high conductivities that rival the best solid-state Zn-ion conductors thus far.

■ ASSOCIATED CONTENT

Supporting Information

The Supporting Information is available free of charge at https://pubs.acs.org/doi/10.1021/jacs.3c10326.

Materials and methods; synthetic procedures; single-crystal X-ray diffraction data, ionic radii and bond metrics, XPS data, PXRD data, TGA data, N_2 sorption data, electrochemical procedures and data. (PDF)

Accession Codes

CCDC 2295993 contains the supplementary crystallographic data for this paper. These data can be obtained free of charge via www.ccdc.cam.ac.uk/data_request/cif, or by emailing data_request@ccdc.cam.ac.uk, or by contacting The Cambridge Crystallographic Data Centre, 12 Union Road, Cambridge CB2 1EZ, UK; fax: +44 1223 336033.

■ AUTHOR INFORMATION

Corresponding Author

Mircea Dincă − *Department of Chemistry, Massachusetts Institute of Technology, Cambridge, Massachusetts 02139, United States;* orcid.org/0000-0002-1262-1264; Email: mdinca@mit.edu

Authors

Andrei Iliescu − *Department of Chemistry, Massachusetts Institute of Technology, Cambridge, Massachusetts 02139, United States;* orcid.org/0000-0002-2076-1566

Justin L. Andrews − *Department of Chemistry, Massachusetts Institute of Technology, Cambridge, Massachusetts 02139, United States*

Julius J. Oppenheim − *Department of Chemistry, Massachusetts Institute of Technology, Cambridge, Massachusetts 02139, United States;* orcid.org/0000-0002-5988-0677

Complete contact information is available at: https://pubs.acs.org/10.1021/jacs.3c10326

Notes

The authors declare no competing financial interest.

■ ACKNOWLEDGMENTS

Ion conductivity and electrochemical measurements were supported by the Brown Science Foundation through the Brown Investigator Award to M.D. Synthetic work was supported by the Department of Energy (DE-SC0023288). We thank Dr. Jiande Wang for useful conversations and assistance with electrochemical measurements.

■ REFERENCES

(1) Wang, F.; Borodin, O.; Gao, T.; Fan, X.; Sun, W.; Han, F.; Faraone, A.; Dura, J. A.; Xu, K.; Wang, C. Highly Reversible Zinc

Metal Anode for Aqueous Batteries. *Nat. Mater.* **2018**, *17* (6), 543−549.
(2) Kundu, D.; Adams, B. D.; Duffort, V.; Vajargah, S. H.; Nazar, L. F. A High-Capacity and Long-Life Aqueous Rechargeable Zinc Battery Using a Metal Oxide Intercalation Cathode. *Nat. Energy* **2016**, *1* (10), 16119.
(3) Pan, H.; Shao, Y.; Yan, P.; Cheng, Y.; Han, K. S.; Nie, Z.; Wang, C.; Yang, J.; Li, X.; Bhattacharya, P.; Mueller, K. T.; Liu, J. Reversible Aqueous Zinc/Manganese Oxide Energy Storage from Conversion Reactions. *Nat. Energy* **2016**, *1* (5), 16039.
(4) Xu, C.; Li, B.; Du, H.; Kang, F. Energetic Zinc Ion Chemistry: The Rechargeable Zinc Ion Battery. *Angew. Chem., Int. Ed.* **2012**, *51* (4), 933−935.
(5) Parker, J. F.; Chervin, C. N.; Pala, I. R.; Machler, M.; Burz, M. F.; Long, J. W.; Rolison, D. R. Rechargeable Nickel−3D Zinc Batteries: An Energy-Dense, Safer Alternative to Lithium-Ion. *Science* **2017**, *356* (6336), 415−418.
(6) Zhang, T.; Tang, Y.; Guo, S.; Cao, X.; Pan, A.; Fang, G.; Zhou, J.; Liang, S. Fundamentals and Perspectives in Developing Zinc-Ion Battery Electrolytes: A Comprehensive Review. *Energy Environ. Sci.* **2020**, *13* (12), 4625−4665.
(7) Zhang, Q.; Luan, J.; Tang, Y.; Ji, X.; Wang, H. Interfacial Design of Dendrite-Free Zinc Anodes for Aqueous Zinc-Ion Batteries. *Angew. Chem., Int. Ed.* **2020**, *59* (32), 13180−13191.
(8) Tang, B.; Shan, L.; Liang, S.; Zhou, J. Issues and Opportunities Facing Aqueous Zinc-Ion Batteries. *Energy Environ. Sci.* **2019**, *12* (11), 3288−3304.
(9) Lv, Y.; Xiao, Y.; Ma, L.; Zhi, C.; Chen, S. Recent Advances in Electrolytes for "Beyond Aqueous" Zinc-Ion Batteries. *Adv. Mater.* **2022**, *34* (4), 2106409.
(10) Xu, X.; Hui, K. S.; Hui, K. N.; Wang, H.; Liu, J. Recent Advances in the Interface Design of Solid-State Electrolytes for Solid-State Energy Storage Devices. *Mater. Horiz.* **2020**, *7* (5), 1246−1278.
(11) Hu, X.; Liu, Q.; Lin, K.; Han, C.; Li, B. The Rise of Metal−Organic Frameworks for Electrolyte Applications. *J. Mater. Chem. A* **2021**, *9* (37), 20837−20856.
(12) Zhao, R.; Wu, Y.; Liang, Z.; Gao, L.; Xia, W.; Zhao, Y.; Zou, R. Metal−Organic Frameworks for Solid-State Electrolytes. *Energy Environ. Sci.* **2020**, *13* (8), 2386−2403.
(13) Kharod, R. A.; Andrews, J. L.; Dincă, M. Teaching Metal-Organic Frameworks to Conduct: Ion and Electron Transport in Metal-Organic Frameworks. *Annu. Rev. Mater. Res.* **2022**, *52* (1), 103−128.
(14) Duan, X.; Ouyang, Y.; Zeng, Q.; Ma, S.; Kong, Z.; Chen, A.; He, Z.; Yang, T.; Zhang, Q. Two Carboxyl-Decorated Anionic Metal−Organic Frameworks as Solid-State Electrolytes Exhibiting High Li^+ and Zn^{2+} Conductivity. *Inorg. Chem.* **2021**, *60* (15), 11032−11037.
(15) Wang, Z.; Hu, J.; Han, L.; Wang, Z.; Wang, H.; Zhao, Q.; Liu, J.; Pan, F. A MOF-Based Single-Ion Zn^{2+} Solid Electrolyte Leading to Dendrite-Free Rechargeable Zn Batteries. *Nano Energy* **2019**, *56*, 92−99.
(16) Zhang, Q.; Liu, B.; Wang, J.; Li, Q.; Li, D.; Guo, S.; Xiao, Y.; Zeng, Q.; He, W.; Zheng, M.; Ma, Y.; Huang, S. The Optimized Interfacial Compatibility of Metal−Organic Frameworks Enables a High-Performance Quasi-Solid Metal Battery. *ACS Energy Lett.* **2020**, *5* (9), 2919−2926.
(17) Bloch, E. D.; Queen, W. L.; Hudson, M. R.; Mason, J. A.; Xiao, D. J.; Murray, L. J.; Flacau, R.; Brown, C. M.; Long, J. R. Hydrogen Storage and Selective, Reversible O_2 Adsorption in a Metal−Organic Framework with Open Chromium(II) Sites. *Angew. Chem., Int. Ed.* **2016**, *55* (30), 8605−8609.
(18) Dinca, M.; Dailly, A.; Liu, Y.; Brown, C. M.; Neumann, D. A.; Long, J. R. Hydrogen Storage in a Microporous Metal−Organic Framework with Exposed Mn^{2+} Coordination Sites. *J. Am. Chem. Soc.* **2006**, *128* (51), 16876−16883.
(19) Sumida, K.; Horike, S.; Kaye, S. S.; Herm, Z. R.; Queen, W. L.; Brown, C. M.; Grandjean, F.; Long, G. J.; Dailly, A.; Long, J. R. Hydrogen Storage and Carbon Dioxide Capture in an Iron-Based Sodalite-Type Metal−Organic Framework (Fe-BTT) Discovered via High-Throughput Methods. *Chem. Sci.* **2010**, *1* (2), 184−191.
(20) Liao, J.-H.; Chen, W.-T.; Tsai, C.-S.; Wang, C.-C. Characterization, Adsorption Properties, Metal Ion-Exchange and Crystal-to-Crystal Transformation of $Cd_3[(Cd_4Cl)_3(BTT)_8(H_2O)_{12}]_2$ Framework, Where BTT^{3-} = 1,3,5-Benzenetristetrazolate. *CrystEngComm* **2013**, *15* (17), 3377−3384.
(21) Dincă, M.; Han, W. S.; Liu, Y.; Dailly, A.; Brown, C. M.; Long, J. R. Observation of Cu^{2+}−H_2 Interactions in a Fully Desolvated Sodalite-Type Metal−Organic Framework. *Angew. Chem., Int. Ed.* **2007**, *46* (9), 1419−1422.
(22) Yang, G.-S.; Li, M.-N.; Li, S.-L.; Lan, Y.-Q.; He, W.-W.; Wang, X.-L.; Qin, J.-S.; Su, Z.-M. Controllable Synthesis of Microporous, Nanotubular and Mesocage-like Metal−Organic Frameworks by Adjusting the Reactant Ratio and Modulated Luminescence Properties of Alq3@MOF Composites. *J. Mater. Chem.* **2012**, *22* (34), 17947−17953.
(23) Dincă, M.; Long, J. R. High-Enthalpy Hydrogen Adsorption in Cation-Exchanged Variants of the Microporous Metal−Organic Framework $Mn_3[(Mn_4Cl)_3(BTT)_8(CH_3OH)_{10}]_2$. *J. Am. Chem. Soc.* **2007**, *129* (36), 11172−11176.
(24) Brozek, C. K.; Cozzolino, A. F.; Teat, S. J.; Chen, Y.-S.; Dincă, M. Quantification of Site-Specific Cation Exchange in Metal−Organic Frameworks Using Multi-Wavelength Anomalous X-Ray Dispersion. *Chem. Mater.* **2013**, *25* (15), 2998−3002.
(25) He, X.; Iliescu, A.; Yang, T.; Arguilla, M. Q.; Chen, T.; Kulik, H. J.; Dincă, M. Reversible O−O Bond Scission and O_2 Evolution at MOF-Supported Tetramanganese Clusters. *J. Am. Chem. Soc.* **2023**, *145* (30), 16872−16878.
(26) Irving, H.; Williams, R. J. P. 637. The Stability of Transition-Metal Complexes. *J. Chem. Soc.* **1953**, No. 0, 3192−3210.
(27) Martinolich, A. J.; Lee, C.-W.; Lu, I.-T.; Bevilacqua, S. C.; Preefer, M. B.; Bernardi, M.; Schleife, A.; See, K. A. Solid-State Divalent Ion Conduction in $ZnPS_3$. *Chem. Mater.* **2019**, *31* (10), 3652−3661.

https://doi.org/10.1021/jacs.3c10326
J. Am. Chem. Soc. 2023, 145, 25962−25965